

ESTUDIO DEL MECANISMO DE FALLA DE TERRAPLENES DEBIDO A LA INFILTRACIÓN DE AGUAS LLUVIAS MEDIANTE EL MONITOREO DE PRESIONES DE POROS Y CONTENIDOS DE AGUA

STUDY OF FAILURE MECHANISM IN EMBANKMENTS INDUCED BY RAINFALL INFILTRATION BY MONITORING PORE WATER PRESSURES AND WATER CONTENTS

EDWIN GARCÍA

Lecturer, Department of Civil Engineering, University of Antioquia, egarcia@udea.edu.co

TARO UCHIMURA

Associate Professor, Department of Civil Engineering, University of Tokyo, uchimura@civil.t.u-tokyo.ac.jp

Recibido para revisar 27 de Julio de 2006, Aceptado 14 de Noviembre de 2006, Version final 24 de Enero de 2007

RESUMEN: El presente artículo muestra experimentos realizados utilizando modelos a escala para estudiar el proceso de infiltración en terraplenes sometidos a aguas lluvias. Varios modelos a escala fueron construidos usando un suelo arenoso con alto contenido de finos; para aplicar la lluvia artificial y observar el proceso de infiltración del agua se utilizó un tubo de irrigación. Para monitorear los cambios en succión ocasionados por los ciclos de humedecimiento y secado se instalaron dentro del suelo varios sensores de presión de poros, contenido de agua y de desplazamiento en diferentes puntos. El cambio de la presión de poros en el tiempo, el contenido de agua y las relaciones entre las mediciones de presión de poros y desplazamientos del suelo son presentados. Este estudio muestra que el movimiento del suelo en un talud está directamente relacionado con el contenido de agua del suelo y las presiones de poros existentes en él, sugiriendo que por medio del monitoreo de estos dos parámetros es posible predecir fallas locales inducidas por infiltración de aguas lluvias en los taludes.

ABSTRACT: This paper presents experiments using scale models to study the infiltration process on embankments subjected to rainfall infiltration. Various model embankments were built using a silty sand soil; an irrigation pipe was used to applied artificial rainfall in order to observe the effect of the water infiltration. Pore water pressure, water content and displacements transducers were installed within the scale models at various locations to monitor the changes in suction caused during cycles of wetting and drying processes. Pore water pressure histories, water content histories and relations between measurements of pore water pressures and displacements are presented. This study showed that slope movements are directly related to the soil water content and pore water pressures within the slope, suggesting that slope failure caused by rainfall infiltration could be predicted by monitoring these parameters.

KEY WORDS: Embankment, unsaturated soils, rainfall effect, rainfall infiltration.

PALABRAS CLAVE: Terraplén, suelos no saturados, efecto lluvia, infiltración de aguas lluvias.

1. INTRODUCTION

Slope failure may be triggered by many natural conditions: earthquakes, rainfalls, volcanic eruptions, snow melting, human activities, etc. Among natural hazards, landslides occur in virtually every country in the world. Globally,

they cause approximately 1000 deaths a year with property damage of about US 4 billion (Orense 2003). Colombia as a tropical country has two rainy seasons during the year (March to May and September to November); during this time heavy rainfall causes considerable damage to highways, serious threats to settlements, transport infrastructure and tourism. Although,

newly constructed embankments are adopted with various soil improvement techniques such as geo-reinforcement and internal drainage facilities, old existing embankments are having poor drainage conditions that lead to instability of the structure with water infiltration. Considering the cost of improvement of all existing embankments, it is worth to understand the stability and the behavior of the embankments during and after rainfall infiltration in order to minimize the damage to the infrastructure and the human casualties caused by the failure of embankments.

To understand how slope failures result from rainfall infiltrations is necessary to study the unsaturated soils. Many times, slope failures occur when the soil is not completely saturated, in such a case, suction (negative pore water pressure) within the soil becomes an important parameter for analyzing the behavior of the soils. Nevertheless, this behavior cannot be explained by the classical soil mechanism, which primary emphasis has been the behavior of dried or saturated soils.

Variation in suction and an increase in pore water pressures reduce the shear strength of soils causing failures; Yoshida et al (1991a, 1991b) and Gallage et al (2005) studied these effects of saturation on the shear strength of soils taken at the landslides sites due to heavy rainfall in recent years. Modeling of scale embankments and monitoring of water contents and negative and

positive pore water pressure within the soil, allow us to understand and to correlate the response of the soils due to the rainfall infiltration in the field with the variation of the strength parameter obtained by laboratory tests.

This paper presents the results of monitored pore-water pressure, monitored water content and lateral displacements at several locations in model slopes during and after an artificial rainfall. Then, the pore-water pressure and water content are plotted against the time to study the drying and wetting processes within the model tests. Infiltration process was explained by the recorded pore water pressures and their distribution. The pore water pressures recorded by two sensors were plotted against lateral displacement in order to show the movement of the soil caused by the water infiltration and the reduction in soil suction. Finally, the contour failures obtained at the final of the test were shown, as well as the pictures of the failure process during the rainfall application.

2. TEST MATERIALS, APPARATUS AND PROCEDURES

2.1 Test materials

In the model tests, two soils were used to construct the embankments. Physical properties of the tested materials are shown in table 1. Figure 1 shows the grain size distribution of the mentioned soils.

Properties	Inage sand	Edosaki sand
Specific gravity – G_s	2.72	2.75
Main grain size – D_{50} (mm)	0.16	0.23
Coefficient of uniformity – C_u	17.86	16.67
Coefficient of gradation – C_g	3.96	4.70
Fines content – (%)	26.47	16.40
Plastic Index	No plastic	No plastic
e_{max}	1.35	1.59
e_{min}	0.84	1.01
Max. Dry unit weight – $\gamma_{d(max)}$ (KN/m^3)	17.00	17.20
Optimum moisture content – w_{opt} (%)	17.56	16.01

Table 1. Physical properties of the tested materials
 Tabla 1. Propiedades físicas de los materiales utilizados

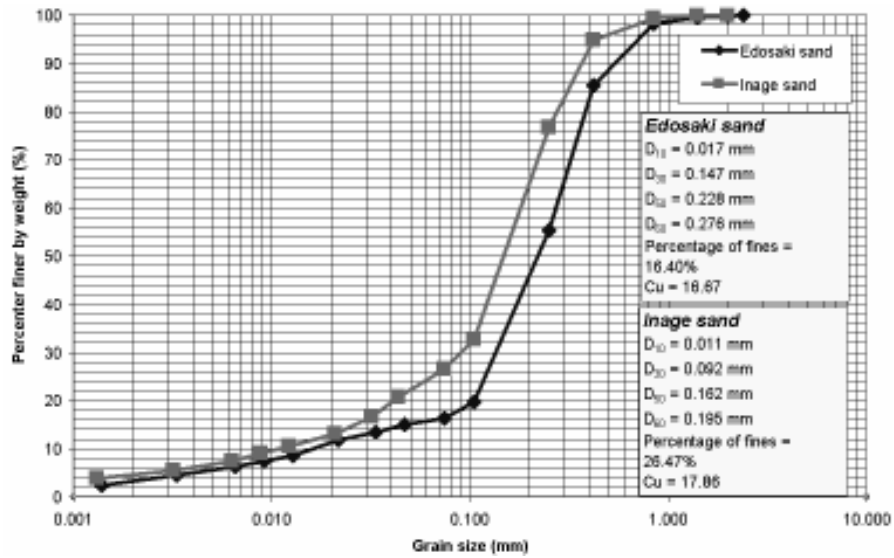


Figure 1. Grain size distribution
 Figura 1. Distribución granulométrica

2.2 Embankment Model and measurement systems

2.2.1 Description

Figure 2 shows the schematic diagram of the soil box and the location of the transducers used for the model embankment No. 1. The major components of the system are: soil box, pore pressure sensors, ceramic cups, water content sensors and rainfall system.

The soil box used in the model test is 220 cm long, 80 cm wide and 100 cm high. The walls of the soil box are made of steel plates, except for the front side which is made of transparent acrylic in order to facilitate the observation of the process. Pore pressure meters and soil moisture content meters were installed within the model embankment. A perforated wall with wired mesh was used at the toe of the embankment in order to allow the free water drainage of the infiltrated water.

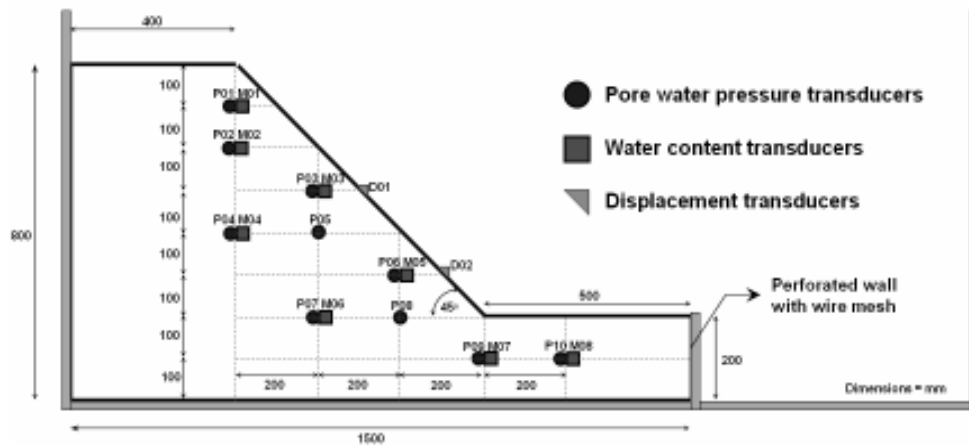


Figure 2. Schematic diagram of model tests and transducer locations
 Figura 2. Diagrama esquemático de los modelos y la localización de los sensores

to achieve good contact between the soil and the ceramic cup, next, a new layer of soil was placed above the sensor. The procedure for placing the moisture content sensor was different; after the pore water pressure sensor was fixed and a new soil layer was placed and compacted, a portion of the soil was removed and the sensor was inserted laterally into the compacted soil.

Rainfall simulation: After preparation of the slope, a spray irrigation pipe was used to simulate artificial rainfall. This pipe produces a fine side spray that simulates constant rainfall. Rainfall intensities of between 40 and 50 mm/hr were simulated using this system. Intensities of

between 80 and 100 mm/hr were achieved using two pipes. The first rainfall was applied during the second day of the tests. After the first rainfall the model embankment was subjected to drying process without rainfall, because the model test was conducted outside the laboratory it was covered with a plastic sheet to avoid the effect of natural rainfall. The models were subjected to a second rainfall in the fourth day. Intensities, durations of the rainfalls and duration of the tests are shown in Table 2. Four burettes were used to measure rainfall intensity, two located at the bottom of the embankment and two at the top.

	Model No. 1	Model No. 2	Model No. 4	Model No. 7
Soil used	Inage sand	Edosaki sand	Edosaki sand	Edosaki sand
Slope degree	45	45	45	45
Initial water content (Average)	12%	18%	11.8%	12.9%
Dry density (g/cm ³)	1.35	1.35	1.20	1.20
Rainfall 1 (mm/hr)	40-50	40-50	40-50	40-50
Duration rainfall 1 (hours)	5	19	2.2	2.5
Rainfall 2 (mm/hr)	40-50	90-100	40-50	40-50
Duration rainfall 2 (hours)	5.5	2	3.2	2.5
Test duration (days)	5	5	4	3
Number of water pressure sensors	10	10	10	17
Number of moisture sensors	8	8	8	10

Table 2. General information and test conditions
 Tabla 2. Información general acerca de los modelos

3. EXPERIMENTAL RESULTS AND DISCUSSION

In order to observe the general pattern of the rainfall infiltration, a series of slope model tests were performed. Artificial rainfall was applied to the model embankments using an irrigation pipe. Pore water pressure transducers to monitor the negative and the positive pore water pressures and water content transducers to measure volumetric water contents, were installed within the model slope at various locations. To measure the displacement of the soil due to the rainfall infiltration, displacement transducers were used in some model tests. All

models responded similarly to the infiltration process.

3.1 Pore water pressure history

Figure 4 shows the time histories of monitored pore water pressure for model test No. 02 (see figure 2 for the location of the transducers). This graph shows that when the first rainfall was applied to the model the negative pore water pressures (suction) started to decrease rapidly. Next, when this rainfall was stopped (drying process), the recorded negative pore water pressures increased, especially in the sensors at the top (sensors P1 to P5). This increment in negative pore water pressure within the soil is

strongly related with the depth of the slope; sensors within the top of the model presented higher suctions than those sensors located at the bottom. This graph also shows that recovering

in suctions is very slow, suggesting that water was retained during a period of time within the soil.

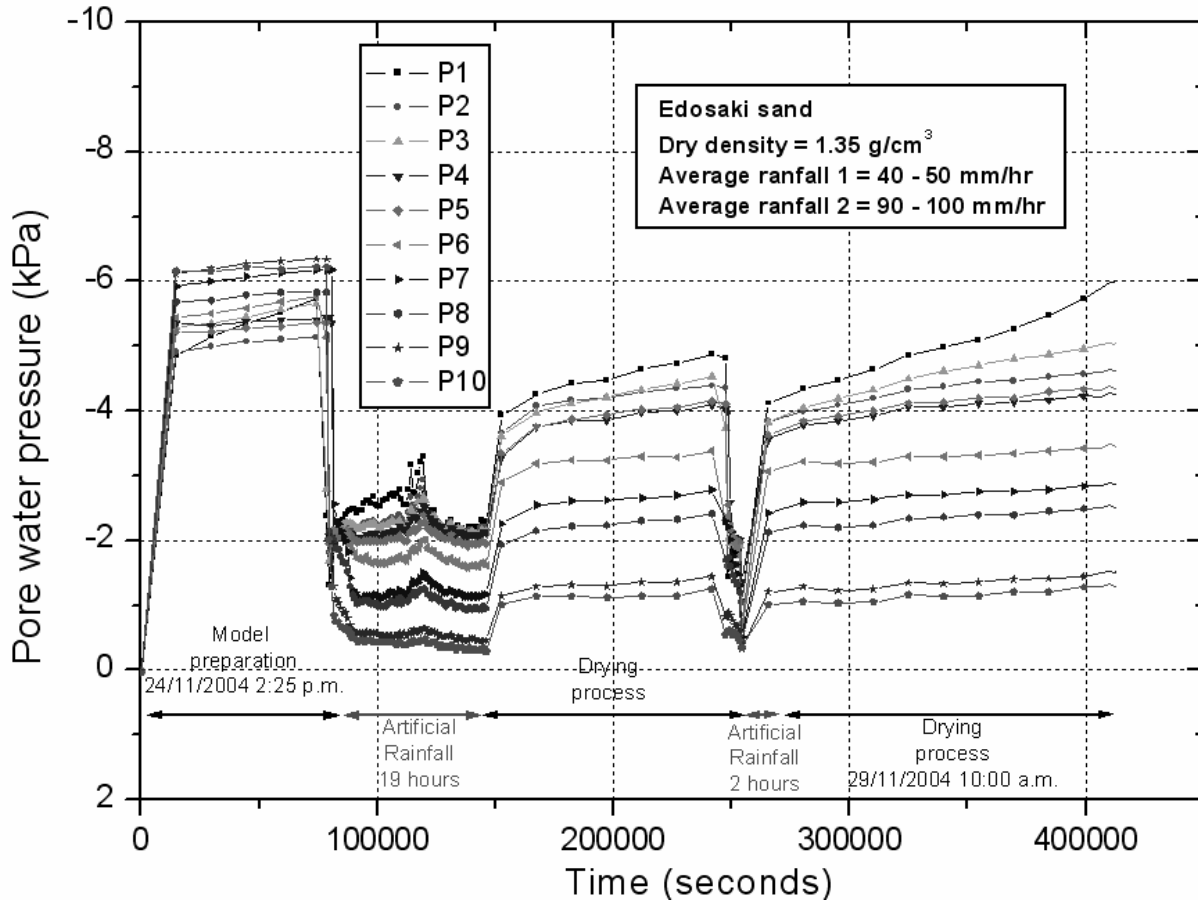


Figure 4. Time histories of pore water pressure model No. 02
Figura 4. Registro histórico de la presión de poros en el modelo No. 02

3.2 Pore water pressure distribution

Monitored pore water pressure distributions for model test No. 2 are shown in figure 5. Four different sketches are shown. At the beginning of the test the model showed uniform pore water pressure in between -5 and -6 kPa (see figure 5.a). Figure 5.b shows the pore water pressure distribution after 18 hours of applying the first rainfall (after 40 hours); suction in the soil reduced to levels in between -1 and -2 kPa and close to zero at the toe of the model. Figure 5.c shows the state of the model when the rainfall was stopped, (drying process, after 68 hours), suction recovered specially at the top of the

model, where the soil reached values similar to those at the beginning of the test, but, at the bottom of the model, lower values of suction were recorded, it can be explained by the accumulation of the water on the bottom of the soil box. Finally, pore water pressure distribution during the second rainfall is shown in figure 5.d (after 71 hours); infiltrated water began to accumulate at the bottom of the model, showing the pore water pressures close to zero after 2 hours of the second rainfall. In all the model tests, water table started to build up from the bottom to the top triggering local retrogressive failure from the bottom of the model.

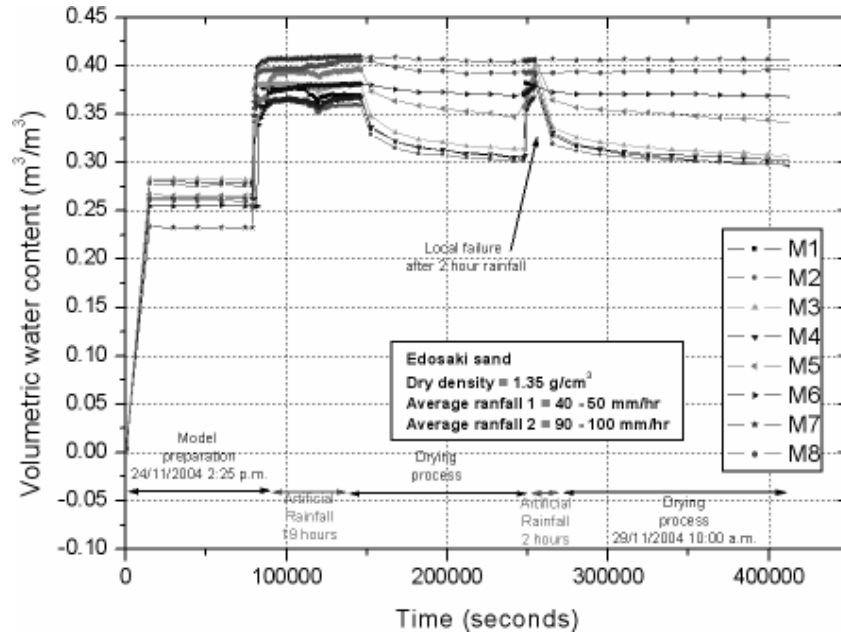


Figure 6. Time history of water content model No. 02
Figura 6. Registro histórico contenido de agua Modelo No. 02

3.4 Horizontal displacement history

Figure 7 shows a picture of the location of the displacement transducers used in the model

embankment No. 7. These devices measured the lateral displacement in the model due to the saturation of the soil.



Figure 7. Transducer configuration to measure displacement. Model Test No. 07
Figura 7. Configuración de los sensores para medir desplazamiento. Modelo No. 07

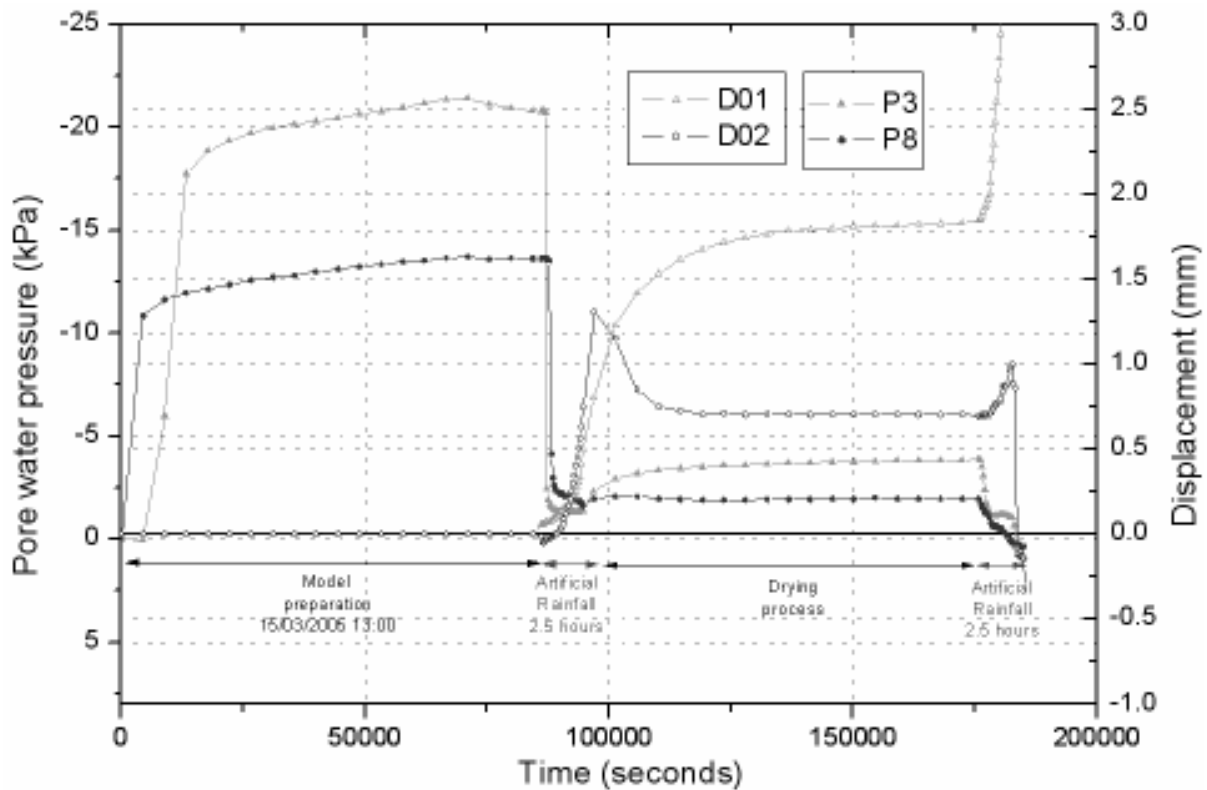


Figure 8. Pore water pressure – Displacement relation. Model No.7
Figura 8. Relación de Presión de poros – Desplazamiento. Modelo No.7

Figure 8 shows the monitored pore water pressure histories of the sensors P3 and P8 and the monitored displacement histories of the transducers D01 and D02 in model test No. 7. Sensors P3 and P8 are the closest sensors to D01 and D02, respectively; the position of the sensor are shown in figure 2. Figure 8 shows that when rainfall 1 was applied, the negative pore water pressures decreased and the lateral displacements increased within the model test; these deformations of the model continue increasing even when the rainfall 1 was stopped; but, they tended to stabilize after some hours. When rainfall 2 was applied, displacement of the soil increased again and once the pore water pressure were positive the model started to fail. It suggests that displacements are strongly related to the growth of water content within the soil. This observation is consistent with the results of triaxial tests on unsaturated specimens, where the most critical parameter in failure initiation was the degree of saturation (Farooq 2002). Monitoring of the water contents within

the soils can predict failure induced by rainfall infiltration. Figure 9 shows the final failure contours of model tests No.4 and No.7. This figure shows that the final contours have similar shape assuring good repeatability of the tests. The tests suggested that failure initiated when water content within the soil increased, especially at the toe of the slope where the soil reaches positive pore water pressures, in contrast, a major portion of the sliding mass may still be in an unsaturated condition. Positive pore water pressure at the toe contributes to the development of highly unstable area at the slope toe which influences on overall instability. This suggests that the effective drainage at the slope toe can prevent progressive sliding due to build up of water table. Tohari et al (2000), observed similar failure mechanism in artificial model slopes, explaining that the saturation process significantly reduced moisture shear strength of the soil, and the increase if water table within the slope decreased the effective stress of the soil, especially at the slope toe.

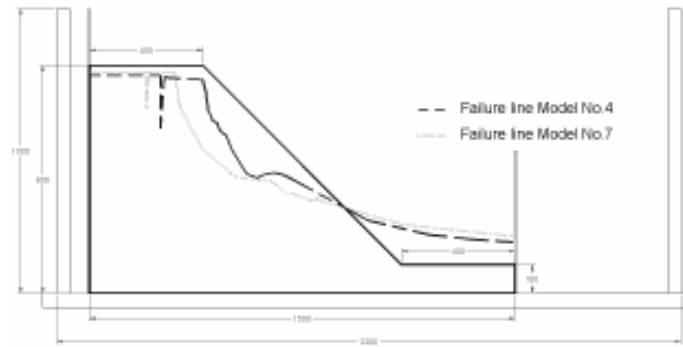


Figure 9. Final contour failure models No. 4 and No. 7
Figura 9. Contorno final de falla Modelos No. 4 y No. 7

3.5 Failure mechanism

Model No. 7 was prepared to be tested at the same conditions of model No. 4. Figure 10 shows some photographs at various stages during the second rainfall. Water infiltrated within the model started to accumulate from the bottom of the slope. Water content and pore water pressure increase at this portion of the model; the effective stress decreased due to the

increment in pore water pressure, until the soil located at the toe reached the failure line. Then, failure progressed due to the continuous saturation. Finally, after progressive failure at the toe, a sliding plane was formed, and the soil mass slipped. As it is showed by the pictures, due to the resulting instability, beginning from the toe of the slope, retrogressive failure occurred.

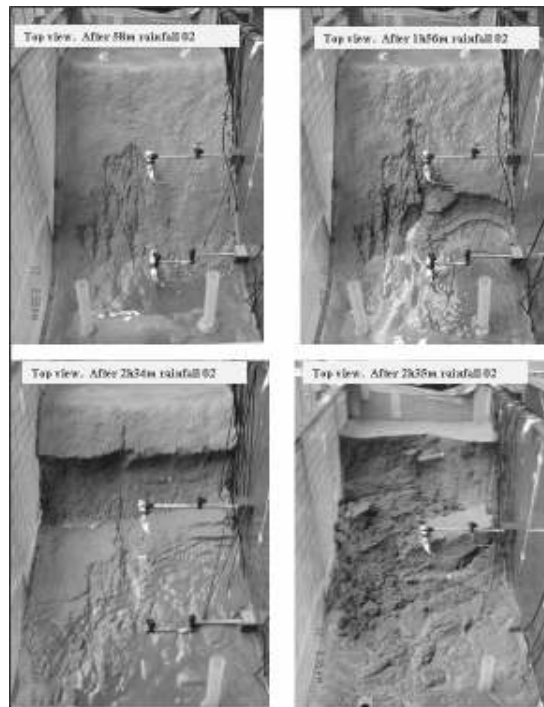


Figure 10. Photographs at various stages. Model No. 07
Figura 10. Fotografías en varias etapas. Modelo No. 07

4. CONCLUSIONS

The tests suggested that failure initiated when water content within the soil increased, especially at the toe of the slope where the soil reaches positive pore water pressures, in contrast, a major portion of the sliding mass may still be in an unsaturated condition.

Soil displacements with the tested embankments are directly related to the soil water contents and pore water pressures within the slopes. The higher the water pressures, the higher the displacements within the soil. Local failure appears at the bottom of the embankments and progressed to the top triggering global failure in the model embankments. Prediction of local and global failure in slopes could be inferred by monitoring water contents and pore water pressures within the soil

5. REFERENCES

- [1] FAROOQ, K. Experimental study on failure initiation in sandy slopes due to rainfall infiltration (PhD thesis). Tokyo, The University of Tokyo, 2002.
- [2] GALLAGE, C.P.K., E.F. Garcia, A. Peiris, T. Uchimura, Use of soil-water characteristic curve in determination of stability of embankments during drying and wetting processes, *Advance Experimental Unsaturated Soil Mechanics*, Experus 2005, Trento, Italy, 351-357, 2005.
- [3] ORENSE, R. P, Geotechnical hazards, nature, assessment and mitigation, The University of The Philippines Press, Philippines, 2003.
- [4] TOHARI, A, Laboratory experiments on initiation of rainfall induced slope failure with moisture content measurements, *GeoEng2000: An International Conference on Geotechnical & Geological Engineering*, Melbourne, Australia, 2000.
- [5] YOSHIDA, Y., J. Kuwano, R. Kuwano, Effects of saturation on shear strength of soils. *Soils and Foundations* 31, No. 1: 181-186, 1991a.
- [6] YOSHIDA, Y., J. Kuwano, R. Kuwano, Rain-induced slope failures caused by reduction in soil strength, *Soil and Foundations* 31, No. 4: 187-93, 1991b.